

Essential Role of Aralar in the Transduction of Small Ca^{2+} Signals to Neuronal Mitochondria*

Received for publication, July 5, 2005, and in revised form, October 26, 2005 Published, JBC Papers in Press, November 3, 2005, DOI 10.1074/jbc.M507270200

Beatriz Pardo^{†1,2}, Laura Contreras^{†1,3}, Antonio Serrano[§], Milagros Ramos[‡], Keiko Kobayashi[¶], Mikio Iijima[¶], Takeyori Saheki[¶], and Jorgina Satrústegui^{‡4}

From the [‡]Departamento de Biología Molecular, Centro de Biología Molecular Severo Ochoa and [§]Centro Nacional de Biotecnología, Consejo Superior de Investigaciones Científicas, Universidad Autónoma de Madrid, 28049 Madrid, Spain and the [¶]Department of Molecular Metabolism and Biochemical Genetics, Kagoshima University, Graduate School of Medical and Dental Sciences, 8-35-1 Sakuragaoka, Kagoshima 890-8544, Japan

Aralar, the neuronal Ca^{2+} -binding mitochondrial aspartate-glutamate carrier, has Ca^{2+} binding domains facing the extramitochondrial space and functions in the malate-aspartate NADH shuttle (MAS). Here we showed that MAS activity in brain mitochondria is stimulated by extramitochondrial Ca^{2+} with an $S_{0.5}$ of 324 nM. By employing primary neuronal cultures from control and aralar-deficient mice and NAD(P)H imaging with two-photon excitation microscopy, we showed that lactate utilization involves a substantial transfer of NAD(P)H to mitochondria in control but not aralar-deficient neurons, in agreement with the lack of MAS activity associated with aralar deficiency. The increase in mitochondrial NAD(P)H was greatly potentiated by large $[\text{Ca}^{2+}]_i$ signals both in control and aralar-deficient neurons, showing that these large signals activate the Ca^{2+} uniporter and mitochondrial dehydrogenases but not MAS activity. On the other hand, small $[\text{Ca}^{2+}]_i$ signals potentiate the increase in mitochondrial NAD(P)H only in control but not in aralar-deficient neurons. We concluded that neuronal MAS activity is selectively activated by small Ca^{2+} signals that fall below the activation range of the Ca^{2+} uniporter and plays an essential role in mitochondrial Ca^{2+} signaling.

Ca^{2+} signaling in mitochondria is mainly achieved through the entry of Ca^{2+} across the Ca^{2+} uniporter, a highly selective Ca^{2+} channel whose identity remains unknown (1, 2). Because of its apparent low affinity for Ca^{2+} , the fact that there is a substantial mitochondrial Ca^{2+} uptake despite modest changes in average $[\text{Ca}^{2+}]_i$ is explained by the strategic location of mitochondria close to the endoplasmic reticulum Ca^{2+} release channels, or plasma membrane Ca^{2+} channels, and therefore to microdomains of very high $[\text{Ca}^{2+}]_i$ (3–6).

In mitochondria, Ca^{2+} activates pyruvate, isocitrate, and α -ketoglutarate dehydrogenases, resulting in an increase in the mitochondrial NADH/NAD ratio (7). The Ca^{2+} uniporter-mitochondrial dehydroge-

nases signaling pathway is very relevant for cell and neuronal function (8–13). However, whether this is the only mechanism to transduce Ca^{2+} signals to mitochondria has never been assessed. In fact, in studies where changes in NAD(P)H, $[\text{Ca}^{2+}]_i$, and $[\text{Ca}^{2+}]_{\text{mit}}$ have been all measured in parallel, it was found that mitochondrial NAD(P)H levels did not closely match those of $[\text{Ca}^{2+}]_{\text{mit}}$ (12, 14–17).

The identification of aralar (alaral1 (18, 19)) as the brain isoform of the Ca^{2+} -dependent aspartate-glutamate mitochondrial carrier (AGC)⁵ SLC25A12 (20) opens up the possibility of an alternative way to transduce Ca^{2+} signals to neuronal mitochondria. Indeed, the Ca^{2+} binding domains of aralar face the mitochondrial intermembrane space, and increases in $[\text{Ca}^{2+}]_i$ result in the activation of aspartate-glutamate exchange, in the absence of calcium entry in mitochondria (20).

The AGCs are one of the transporters responsible for the malate-aspartate NADH shuttle (MAS). Because of the electrogenic nature of Asp/Glu exchange (20, 21), the AGC reaction is irreversible under physiological conditions and thus a potential site for regulation. The first aim of this work was to explore the potential of aralar as a brain AGC isoform to regulate MAS activity in brain at low Ca^{2+} concentrations, below those required for the function of the mitochondrial Ca^{2+} uniporter. MAS activity in brain mitochondria was found to have Ca^{2+} -activation properties adequate for this purpose.

The second aim of this work was to study the role of the aralar-MAS pathway in the supply of reducing equivalents to neuronal mitochondria. Aralar is expressed postnatally in rat and mouse brain, and it is located in neurons. Both MAS activity and aralar expression are acquired in parallel during neuronal maturation (22, 23). Aralar is important for neuronal function as underscored by the finding that alterations in aralar gene and protein are associated with central nervous system diseases such as Mohr-Tranebjærg syndrome, in which there is an impaired targeting of aralar to mitochondria (24), and autism (25). Aralar null mice also exhibit prominent motor coordination defects along with deficient myelination (26).

We have employed primary neuronal cultures from control and aralar-deficient mice (26) and two-photon excitation microscopy imaging of NAD(P)H to monitor the transfer of reducing equivalents from cytosol to mitochondria. We show that MAS is the main pathway to transfer reducing equivalents to neuronal mitochondria. High $[\text{Ca}^{2+}]_i$ signals activate the Ca^{2+} uniporter-mitochondrial dehydrogenases signaling pathway, whereas small $[\text{Ca}^{2+}]_i$ signals selectively activate MAS activity in neurons. We conclude that the aralar-MAS pathway plays an

* This work was supported in part by Dirección General de Investigación del Ministerio de Ciencia y Tecnología Grant BMC2002-02072, Comunidad de Madrid Grant 08.5/0024/2003, Fondo de Investigaciones Sanitarias del Ministerio de Sanidad y Consumo 01/0395 (to J. S.), an institutional grant from the Fundación Ramón Areces to the Centro de Biología Molecular 'Severo Ochoa,' and by a Grant-in-aid for Scientific Research 16390100 from the Japan Society for the Promotion of Science (to K. K.). The costs of publication of this article were defrayed in part by the payment of page charges. This article must therefore be hereby marked "advertisement" in accordance with 18 U.S.C. Section 1734 solely to indicate this fact.

[†] Both authors contributed equally to this work.

² Recipient of a postdoctoral contract from the Comunidad de Madrid.

³ Recipient of a fellowship from the Comunidad de Madrid.

⁴ To whom correspondence should be addressed: Dept. de Biología Molecular, Centro de Biología Molecular Severo Ochoa, Facultad de Ciencias, Universidad Autónoma, 28049 Cantoblanco, Madrid, Spain. Tel.: 34-91-397-4872; Fax: 34-91-397-4799; E-mail: jsatrustegui@cbm.uam.es.

⁵ The abbreviations used are: AGC, aspartate/glutamate carrier; MAS, malate-aspartate NADH shuttle; MSK, mannitol/sucrose/ K^+ medium; LM, lactate + malate; IP₃, inositol 1,4,5-trisphosphate; BSA, bovine serum albumin; MOPS, 4-morpholinepropanesulfonic acid; ANOVA, analysis of variance; mit/cyt, mitochondrial/cytosolic; RR, ruthenium red; α -KGDH, α -ketoglutarate dehydrogenase; α -KG, α -ketoglutarate.

Aralar Transduces Small Ca^{2+} Signals to Mitochondria

essential role to transduce small $[\text{Ca}^{2+}]_i$ signals into neuronal mitochondrial energization.

MATERIALS AND METHODS

Animals—Male Wistar rats (3 months old) were used to prepare rat brain and skeletal muscle mitochondria. SVJ129/C57BL mice carrying a deficiency for aralar expression, *Aralar*^{-/-}, *Aralar*^{+/-}, and *Aralar*^{+/+}, which had been obtained from Lexicon Genetics Inc. (The Woodlands, TX) (26), were used to obtain primary neuronal cultures.

Genotypes—Genotype was determined by PCR using genomic DNA obtained from tail or embryonic tissue samples (Nucleospin tissue kit, Macherey-Nagel). The following primers were used for genomic DNA amplification: sense primer mAra3' LTRF3 (5'-GTTCTCTAGAACTGCTGAGG-3') that detects only mutated alleles, sense primer mAra int 13F1 (5'-GATGTGAGAACTCACCAGTGT-3') that detects wild-type alleles, and antisense primer mAra int 13B (5'-AC-CACCACCAGCGTGTGACG-3') that detects both wild-type and mutant alleles (data not shown). PCR mixtures were preincubated at 94 °C for 5 min, followed by 35 cycles of DNA amplification at 94 °C for 60 s, 58 °C for 60 s, and 72 °C for 60 s; the process was finished with an incubation at 72 °C for 5 min. Wild-type (271 bp) and mutant (406 bp) fragments were separated by electrophoresis on a 1.5% agarose gel.

Isolation of Brain and Skeletal Muscle Mitochondrial Fractions—Whole rat brains were homogenized in 250 mM sucrose, 25 mM Hepes, 10 mM KCl, 1 mM EDTA, 1 mM EGTA, 1.5 mM MgCl_2 , 1 mM dithiothreitol, 1 mM phenylmethylsulfonyl fluoride, 1 mM iodoacetamide, and 0.1% BSA (w/v), pH 7.4 (1:10 w/v). Nuclei and cell debris were first removed by 10 min of centrifugation at $700 \times g$, and mitochondrial fractions were then spun down (15 min, $10,000 \times g$) and washed in 75 mM mannitol, 25 mM sucrose, 5 mM potassium phosphate, 20 mM Tris-HCl, 0.5 mM EDTA, 100 mM KCl, 0.1% BSA, pH 7.4 (mannitol/sucrose/ K^+ medium, MSK). Brain mitochondrial fractions were suspended in the same medium (10–20 mg protein/ml) and corresponded to crude preparations containing synaptosomes and free mitochondria (27).

Rat skeletal muscle mitochondria were obtained as described by Rolfe *et al.* (28) and suspended in MSK until used. Respiration rates were determined with a Clark-type oxygen electrode. Skeletal muscle mitochondria (0.1 to 0.2 mg protein) were added to 0.5 ml of MSK, and different Ca^{2+} concentrations and the respiration rate in the presence of 5 mM glutamate + 5 mM malate + 0.5 mM ADP was recorded. The free Ca^{2+} concentrations in each media was determined with fura-2 or Ca^{2+} -Green as indicated below.

Reconstitution of MAS Activity in Brain Mitochondria—The reconstitution of MAS is described in Jalil *et al.* (26). Briefly, mitochondrial fractions (0.1 to 0.15 mg protein) were suspended in 3 ml of MSK and 100 μM digitonin, and the shuttle was reconstituted in the presence of 4 units/ml glutamate-oxaloacetate transaminase, 6 units/ml malate dehydrogenase, 66 μM NADH, 5 mM aspartate, 5 mM malate, 0.5 mM ADP, 200 nM ruthenium red, and appropriate CaCl_2 additions. The reaction was started by the addition of 5 mM glutamate, was determined from the decay in NADH fluorescence (excitation at 340 nm, emission at 465 nm), and was calibrated with appropriate NADH standards. The free Ca^{2+} concentrations at each Ca^{2+} addition were determined fluorimetrically with fura-2 (below 1 μM free Ca^{2+}) and Ca^{2+} -Green (above 1 μM free Ca^{2+}). The concentrations of fura-2 ($K_d = 224$ nM; excitation, 340 and 380 nm; emission, 510 nm) and Ca^{2+} -Green ($K_d = 14$ μM ; excitation, 506 nm; emission, 532 nm) were 5 and 0.1 μM , respectively. The free Ca^{2+} concentration was obtained by established procedures for ratiometric or nonratiometric probes (29).

To test the effect of intramitochondrial Asp on shuttle activity, mitochondria were preloaded with Asp following published procedures (21). To this end, digitonin-permeabilized mitochondrial fractions were first suspended (16 mg of protein/ml) in a glutamate-containing medium (100 mM potassium glutamate, 100 mM sucrose, 10 mM Tris, 0.1% BSA, pH 7.4) for 10 min at 0 °C to allow for glutamate accumulation in mitochondria. Then the suspension was diluted 1:10 in 320 mM sucrose, 1 mM EDTA, 0.1% BSA, 10 mM Tris, pH 7.4, and centrifuged ($10,000 \times g$, 5 min). Glutamate-loaded mitochondria were washed with the same medium and resuspended (7 mg of protein/ml) in an Asp-loading medium (150 mM KCl, 10 mM MOPS, 0.1% BSA, pH 7.4). Asp loading was started by adding 3 mM oxaloacetate, and after 3 min at 28 °C, the incubation was stopped (0 °C, 5 min of centrifugation at $10,000 \times g$). Asp-loaded mitochondria were washed with Asp-loading medium and resuspended in MSK to assay MAS activity.

Ca^{2+} uptake in brain and muscle mitochondria preparations was measured in the presence of 0.1 μM Ca^{2+} -Green 5N (excitation 506 nm, emission 532 nm) in modified MSK (without EDTA and supplemented with 1 mM MgCl_2). Experiments were performed at 25 °C under constant stirring, with ADP (0.2 mM), glutamate (5 mM), and malate (5 mM) as respiratory substrates. Measurements were started by the addition of mitochondria (to a final concentration of 0.5 mg/ml protein; not shown). After 4 min of preincubation, a first addition of Ca^{2+} (50 μM) was made, followed by sequential additions of 20 μM Ca^{2+} as indicated. Where appropriate, 200 nM ruthenium red was added.

Neuronal Cultures—Cortical neuronal cultures were prepared from 16-day-old mouse embryos, following the procedure used for rat embryos (23, 30) modified as follows. Mouse embryos were obtained from crosses between SVJ129/C57BL6 *Aralar*^{+/-} mice, and nonbrain tissue was used for determination of DNA genotype of every embryo. Because the number of *Aralar*^{+/-} embryos doubled that of *Aralar*^{+/+}, *Aralar*^{+/-} mice were employed as controls, unless indicated otherwise. Cerebral cortices were removed free of meninges, cut into small pieces, and enzymatically dissociated in phosphate-buffered saline containing 1% BSA, 0.4 mg/ml papain, and 6 mM glucose and then mechanically dissociated, in the presence of DNase, by using glass pipettes of different pore size. Dissociated cells were collected by centrifugation ($800 \times g$, 5 min) and seeded in medium containing 20% horse serum for 3 h. After this time, medium was completely replaced with serum-free B27-supplemented Neurobasal medium (31). The culture medium was partially replaced every 2nd day. Cells were plated at a density of 1×10^5 cells/cm² on poly-L-lysine and laminin-coated pretreated glass coverslips for the determination of $[\text{Ca}^{2+}]_i$ (30), or on glass coverslips sealed at the bottom of plastic wells (4-well LabTek cover slides, NUNC, Roskilde, Denmark), for two-photon microscopy. The different cell types in these neuronal cultures were characterized with specific antibodies as described earlier (30, 32). Under the present culture conditions, neurons represented more than 90% of the total cell population. Cultures were used for experimentation between 9 and 11 days *in vitro*.

Two-photon Microscopy in Neuronal Cultures—Neuronal cultures, seeded on 4-well LabTek cover slides, were washed once and incubated in glucose-free HCSS (1 mM CaCl_2 , 120 mM NaCl, 0.8 mM MgCl_2 , 25 mM Hepes, 5.4 mM KCl, pH 7.4) for 1 h before experimentation. When Ca^{2+} -free conditions were needed, cells were washed once and maintained with Ca^{2+} -free HCSS in the presence of 100 μM EGTA.

Two-photon excitation microscopy was performed by using Olympus IX70 inverted microscope with an $\times 60$ Plan Apo NA 1.4 objective, coupled to a Bio-Rad Radiance 2000 MP confocal/multiphoton microscopy system. An infrared multiphoton laser (Coherent Mira 690–1000 nm) provided excitation of intrinsic NADH fluorescence. The laser set-

tings used for imaging were as follows: 4 milliwatts of power, with a neutral filter set to reduce the excitation light in 80%, and long wave at 735 nm with 150-fs pulses. Images were collected with a 390–460 nm emission filter. Cells were maintained at 37 °C with a temperature-controlled microscopic stage. Additions (0.1 ml) were made as a bolus to the cell chamber (initial volume, 0.5 ml).

Images (averages of three frames, 512×512 pixels per frame, $0.4 \mu\text{m}/\text{pixel}$) were taken every 5 or 10 s for about 2–5 min. Image analysis was carried out with MetaMorph (Universal Imaging). Mitochondrial and cytosolic intensities were determined in individual cells or groups of cells following procedures used in islet beta cells (33, 34). Because of their movement in and out of the focal plane, a particular mitochondria may not be imaged at all time points. Thus, the analysis was carried out only on those mitochondria that stood in the focal plane at each time point. Selected regions (with 4–10 cells) or individual cells were outlined, and intensity thresholds were set that highlighted the bright areas shown to correspond to in-focus mitochondria (from Mitotracker labeling, see below). With these thresholds, which may underestimate the mitochondrial fluorescence but avoid contamination from the cytoplasmic compartment, the intensity of these bright areas was calculated. To estimate the cytoplasmic fluorescence, intensity thresholds were set in order to include the dim areas within cells and to exclude mitochondrial fluorescence. This probably entails an overestimation of the cytosol because of the dense neurite network where neurites and background are hard to tell apart.

Changes in NAD(P)H fluorescence were then calculated as mitochondrial/cytosolic (mit/cyt) NAD(P)H ratios or as normalized fluorescence values (cyt/cyt_0 , mit/mit_0). By using a more restrictive estimation of the cytosol, mit/cyt NAD(P)H ratios were increased, but the differences between genotypes or stimuli were maintained.

In each case, measurements to determine changes in NAD(P)H autofluorescence were performed in at least three independent experiments. Statistical significance was calculated for every experimental condition (genotype and/or stimuli applied) by using time course data sets of mit/cyt NAD(P)H fluorescence ratios and one-way analysis of variance (ANOVA). Thereafter, time courses for mit/cyt NAD(P)H fluorescence ratios obtained from different genotypes or stimuli were compared by a two-factor ANOVA test. The statistically significant results of the previous comparisons are indicated in the figure legends. In addition, data at the indicated time points were used to calculate the reducing equivalent transfer ratio (quotient between maximum and initial mit/cyt NAD(P)H ratios) and were analyzed for significance (unpaired two-tailed *t* test or Bonferroni's test).

To label mitochondria with MitoTracker, neurons were first incubated with lactate and malate to reduce mitochondrial NAD(P)H. After capturing the NAD(P)H fluorescence images, they were then incubated for 15 min with 100 nM MitoTracker Red CMXRos (Molecular Probes) on the microscope stage, where confocal images were captured using a He-Ne laser (543 nm excitation) and a 560–600 nm emission filter (resolution, $0.16 \mu\text{m}/\text{pixel}$).

Pyruvate Determination—Pyruvate content was measured in the neuronal cultures exposed to the same experimental conditions used for two-photon microscopy. To measure pyruvate content, cells were washed once and incubated for 1 h in glucose-free HCSS and were then incubated for 3 min in glucose- and Ca^{2+} -free HCSS (100 μM EGTA) with 20 mM lactate and 5 mM malate. Cells were placed on ice, washed with cold phosphate-buffered saline, and scraped into 0.5 N perchloric acid. Deproteinized cellular pellets obtained in this way were lyophilized. Pyruvate content in these samples were spectrofluorimetrically measured by a standard enzymatic end points method (35).

Determination of $[\text{Ca}^{2+}]_i$ and $[\text{Ca}^{2+}]_{\text{mit}}$ in Neuronal Cultures—It was determined that $[\text{Ca}^{2+}]_i$ neurons were grown on coverslips and loaded with fura-2AM by incubation in Ca^{2+} -free HCSS with 5 μM fura-2AM and 50 μM pluronic acid (Molecular Probes), for 20 min at 37 °C, and rinsed with HCSS, 1 mM CaCl_2 , for 30 min. The $[\text{Ca}^{2+}]_i$ was then determined by Ca^{2+} imaging as described before (30).

To determine $[\text{Ca}^{2+}]_{\text{mit}}$, cells were loaded with rhod-2 as described previously (15). Cortical neurons were incubated at 4 °C for 15 min in HCSS containing 4 μM rhod-2 AM. The dye-containing buffer was then replaced by culture medium and incubated overnight at 37 °C, under 95% air and 7% CO_2 , to dissipate any cytosolic dye. The combination of cold loading, to decrease the activity of intracellular cytosolic esterases, and the cationic properties of rhod-2 allowed a preferential accumulation of the dye into mitochondria.

Rhod-2-loaded neurons were preincubated exactly under the same conditions used for two-photon microscopy, mounted on the stage of a confocal laser scanning (LSM510META) microscope (Axiovert 200, Zeiss), and imaged using a $40\times$ oil Plan-Neofluar objective (1.3 NA) and an additional digital magnification of $1.2\times$. Images were obtained upon illumination with a helium-neon laser at 543 nm, and the emitted light was recorded with a 560 nm long-pass filter. Images (averages of 200 frames: 512×512 pixels, $192 \mu\text{m} \times 192 \mu\text{m}$) were acquired with a confocal slit aperture setting of $72 \mu\text{m}$, once every 5 s. Confocal images were analyzed with MetaMorph software (Universal Imaging). To study the variations of Ca^{2+} concentrations in mitochondria in single neurons, individual cells were outlined manually, and the variations in fluorescence were expressed as F/F_0 , where F is the emitted fluorescence at any given time, and F_0 is the fluorescence of the same zone at time = 0.

RESULTS

Ca^{2+} Activation of the Malate-Aspartate NADH Shuttle in Brain Mitochondria—MAS activity in brain mitochondria, measured as a decrease in NADH in the incubation medium, was dependent upon Glu addition, and under our assay conditions, it did not require Asp-preloading of mitochondria (Fig. 1, A and B). MAS activity was completely absent in brain mitochondrial fractions from *Aralar*^{−/−} mice (26). In addition, respiration on glutamate plus malate was extremely reduced in skeletal muscle mitochondria with no compensatory increase in respiration with pyruvate plus malate (26). Similarly, the lack of citrin, the liver AGC isoform, is not accompanied by compensatory increases in the activity of the glycerol phosphate NADH shuttle (36).

To study Ca^{2+} activation of MAS, shuttle activity was measured after the addition of calibrated Ca^{2+} loads in the presence of 200 nM ruthenium red (RR) to block Ca^{2+} uptake through the Ca^{2+} uniporter. Under these conditions, any activation of the shuttle can be attributed to the effect of Ca^{2+} on the external face of the inner mitochondrial membrane, where the Ca^{2+} binding domains of aralar are located (20).

Fig. 1, C and D, shows that MAS activity increased with Ca^{2+} . The maximal activation was about 3.1-fold (from 26.7 ± 5.28 to 85.18 ± 10.4 nmol \times mg protein^{−1} \times min^{−1}, in the absence of Ca^{2+} or at saturating Ca^{2+} concentrations, respectively) with an $S_{0.5}$ of 324 ± 114 nM. A similar increase in activity (2.55 ± 0.57 -fold) was observed when the assay was carried out with aspartate-preloaded mitochondria. The $S_{0.5}$ value for Ca^{2+} activation is substantially lower than that of the Ca^{2+} uniporter of mitochondria (apparent K_m about 10–20 μM (2, 37)), suggesting that Ca^{2+} activation of the shuttle may contribute to NADH reduction in mitochondria at Ca^{2+} concentrations where the Ca^{2+} uniporter is still inactive.

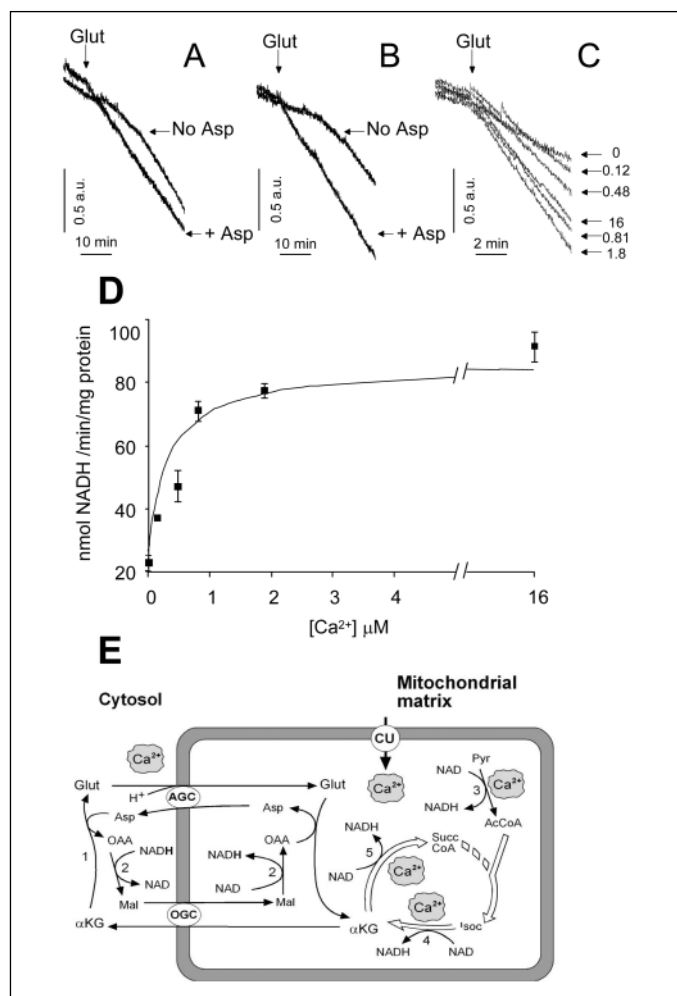


FIGURE 1. Ca^{2+} activation of the MAS activity in brain mitochondria. A and B, MAS activity in rat brain mitochondrial preparations subjected to aspartate-preloading (B) or under control conditions (A) assayed in the presence (+ Asp) or absence (No Asp) of 5 mM aspartate. 5 mM glutamate (Glut) is added where indicated. The presence of Asp in the external medium reduced the time lag required to obtain the maximal slope (compare traces No Asp and + Asp in A and B) but did not modify the final activity obtained (compare final slopes in A and B). Asp-preloading did not change the activity of the shuttle (compare traces + Asp in A and B). C, MAS activity at the free Ca^{2+} concentrations (μM) indicated. Traces in A–C correspond to representative experiments. D, kinetics of Ca^{2+} activation of MAS activity. Data are mean \pm S.E. of three experiments performed in triplicate. E, Ca^{2+} activation of malate-aspartate NADH shuttle and mitochondrial dehydrogenases. See “Discussion” for details. AcCoA, acetyl-CoA; CU, Ca^{2+} uniporter; Glut, glutamate; Isoc, isocitrate; αKG , α -ketoglutarate; Mal, malate; OAA, oxalacetic acid; OGC, α -ketoglutarate/malate carrier; Pyr, pyruvate; SuccCoA, succinyl-CoA; step 1, aspartate aminotransferase (AAT); step 2, malate dehydrogenase (MDH); step 3, pyruvate dehydrogenase (PDH); step 4, isocitrate dehydrogenase (IDH); step 5, α -KGDH.

Two-photon Measurement of Lactate-induced Changes in NAD(P)H in Cultured Neurons—Primary cortical neuronal cultures from *Aralar*^{+/−} mouse embryos used as control were equilibrated with glucose-free HCSS for 1 h and then switched to glucose- and Ca^{2+} -free HCSS, 100 μM EGTA, to start autofluorescence imaging. After acquiring 2 images (one every 10 s), 20 mM lactate + 5 mM malate (LM) was added to the incubation chamber, and fluorescence was recorded for 2–5 min.

The total fluorescence of the neurons (average of 30 cells) increased markedly after LM addition (Fig. 2, A and B), and this increase was not observed when vehicle was added (Fig. 2A), indicating that it was LM-dependent. There were hardly any changes in total, mitochondrial, or cytosolic fluorescence in vehicle-exposed neurons (Fig. 2A and data not shown), indicating that photobleaching in these experiments was very low.

At the subcellular level, autofluorescence was found to concentrate in bright punctate regions stained with Mitotracker (Fig. 2B) that were presumed to be mitochondria. The LM-induced increases in fluorescence of mitochondria, and the neighboring cytoplasm, are represented in Fig. 2, C–F. As observed, the addition of LM resulted in an increase in the two regions, with individual variation of the responses among cells (Fig. 2, C and E). This was expected because lactate entering the cells via neuronal monocarboxylate carriers (38) would immediately increase the cytosolic NADH/NAD level through the lactate dehydrogenase reaction. However, mitochondria had the greatest increase in NAD(P)H fluorescence (note the different scales). We have not quantified the actual increase in NAD(P)H in mitochondria or cytosol, because it may involve both free but mostly bound NAD(P)H, and the fluorescence of these two forms is very different, about 10-fold higher when bound (39, 40).

In order to test that cytosolic and mitochondrial fluorescence signals were adequately separated in the imaging experiments, we studied the response to rotenone, which has selective effects on mitochondrial NAD(P)H. Fig. 2G shows that rotenone addition results in a very large increase in normalized mitochondrial fluorescence, with no changes in cytoplasmic fluorescence, indicating that contamination between mitochondrial and cytosolic signals is below detection in our current set up.

Lack of Increase in Mitochondrial NAD(P)H in Response to Lactate in Aralar-deficient Neurons—To study the role of aralar, the response to LM addition was studied in control and aralar-deficient neuronal cultures derived from littermate embryos in Ca^{2+} -free media and in the presence of 1 mM Ca^{2+} . Fig. 3A shows the changes in the mit/cyt NAD(P)H fluorescence ratio in response to LM (added at the arrow) in Ca^{2+} -free media. The changes in normalized mitochondrial fluorescence ratio are shown in Fig. 3B. Control neurons showed varied responses to LM and reached a plateau at about 1 min after LM addition (Fig. 3A). In contrast, neurons from aralar-deficient mice showed a very modest rise in both the mit/cyt and normalized mitochondrial fluorescence ratio (Fig. 3, A and B). These changes were essentially the same in the presence of Ca^{2+} . In fact, the reducing equivalent transfer (see “Materials and Methods”) was not statistically different in the presence of 1 mM Ca^{2+} or in Ca^{2+} -free media both in control ($n = 30$ –180 neurons, $p > 0.6$) and aralar-deficient neurons ($n = 30$ –180, $p > 0.8$). $[\text{Ca}^{2+}]_i$ was not modified by LM addition either in the absence or presence of Ca^{2+} (results not shown), indicating that MAS activity is activated solely by the rise in cytosolic NADH obtained upon lactate entry.

Lactate gives rise to pyruvate through lactate dehydrogenase. Therefore, the increase in mitochondrial NAD(P)H may be due to NADH shuttle activity and to the entry and oxidation of pyruvate in mitochondria. To determine the contribution of lactate-derived pyruvate oxidation in the increase in mitochondrial NAD(P)H, we have studied the responses to pyruvate plus malate in control and aralar-deficient neurons. Two and 10 mM (not shown) pyruvate (plus 5 mM malate) induced concentration-dependent increases in the mit/cyt NAD(P)H fluorescence ratio, which were similar in control and aralar-deficient neurons (Fig. 3C).

Because the responses to pyruvate and the internal pyruvate concentrations observed 2 min after LM addition (nmol/ 5×10^6 cells) were the same in control (0.79 ± 0.09) and aralar-deficient (1.08 ± 0.18) neurons, the blunted response to LM caused by aralar deficiency is clearly due to a decreased transfer of reducing equivalents from cytosolic NADH to mitochondria. Although a small and nonsignificant increase in cytosolic NAD(P)H fluorescence has been observed in aralar-deficient neurons (results not shown), its contribution to the blunted response to LM is probably a minor one, as the changes in mitochondrial/cytosolic or

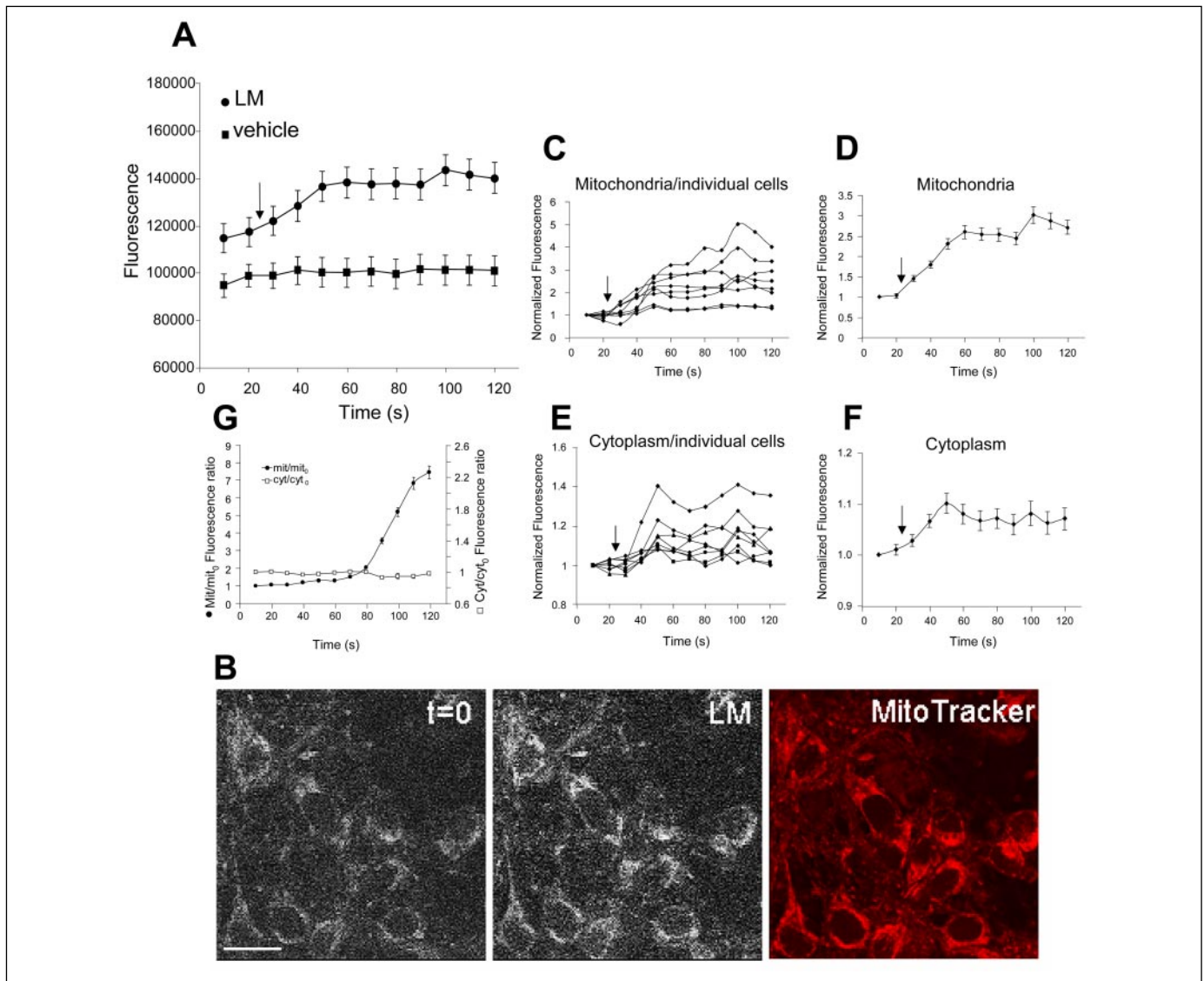


FIGURE 2. NAD(P)H autofluorescence measured by two-photon excitation microscopy in neuronal cell cultures. Neuronal cell cultures from embryonic cortex of control, *Aralar*^{+/−} mice were preincubated in glucose-free HCSS, 1 mM CaCl_2 for 1 h at 37 °C and then switched to Ca^{2+} - and glucose-free HCSS (100 μM EGTA). The initial autofluorescence of the cells revealed only a few bright spots per cell that corresponded to in-focus mitochondria. **A**, total NAD(P)H autofluorescence in 30 individual cells was registered before (20 s) and after 20 mM lactate plus 5 mM malate (LM) or vehicle (Ca^{2+} -free HCSS; $n = 15$ cells) addition, as indicated by the arrow. Images were acquired every 10 s. **B**, NAD(P)H images of selected neurons immediately before ($t = 0$) and after 90 s of stimulation with LM and after MitoTracker Red CMXRos staining. Bar represents 20 μm . **C–F**, changes in normalized (F/F_0) mitochondrial and cytoplasmic NAD(P)H autofluorescence in eight individual cells (**C** and **E**) and mean \pm S.E. values of 30 cells (**D** and **F**). LM addition is indicated by the arrow. **G**, changes in normalized mitochondrial (mit/mit_0) and cytoplasmic (cyt/cyt_0) fluorescence ratio in neuronal cultures exposed to 2 μM rotenone at $t = 0$.

normalized mitochondrial fluorescence ratios are the same (Fig. 3, *A* and *B*).

Reducing equivalent transfer at 70 s after LM addition in Ca^{2+} -free medium (quotient between mit/cyt NAD(P)H ratios at 70 s and initial values) was 1.76 ± 0.03 in control and 1.3 ± 0.01 in *aralar*-deficient neurons (mean \pm S.E. of 72–180 neurons, $p < 0.0001$; ANOVA followed by unpaired two-tailed t test). Similar results were obtained in the presence of 1 mM Ca^{2+} (reducing equivalent transfer was 1.82 ± 0.11 and 1.29 ± 0.16 , in control and *aralar*-deficient neurons, $n = 30$ –100 neurons, $p < 0.05$, unpaired t test). The contribution to this increase of pyruvate (lactate-derived) oxidation can be estimated from the values in *aralar*-deficient neurons, and it represents about 40% of the increase, with MAS activity corresponding to the remaining 60%. It is unlikely that glycerol 3-phosphate shuttle activity contributes significantly to this process, because it is relatively small in neurons (41). It donates electrons to complex III, and any change in mitochondrial NAD(P)H

level from that activity would depend on reverse electron transport. Thus, MAS activity is a major pathway for lactate-dependent reduction of mitochondrial NAD(P)H in control neurons.

Regulation of Mitochondrial NAD(P)H Response by Large Ca^{2+} Signals—By having established that lactate-induced increase in reducing equivalent transfer to mitochondria is mostly due to MAS activity, we sought to determine the role of $[\text{Ca}^{2+}]_i$ in the regulation of shuttle activity.

To this end, we have studied the increase in mitochondrial NAD(P)H in neurons in response to two types of Ca^{2+} signals as follows: large $[\text{Ca}^{2+}]_i$ signals brought about by depolarization-dependent activation of voltage-operated Ca^{2+} channels in the presence of millimolar external Ca^{2+} concentrations, and small $[\text{Ca}^{2+}]_i$ signals, generated in a Ca^{2+} -free medium by Ca^{2+} mobilization via activation of IP_3 receptors. In the first case, in addition to Ca^{2+} -mediated MAS activation, it was expected that voltage-operated Ca^{2+} channel-dependent Ca^{2+} entry would result

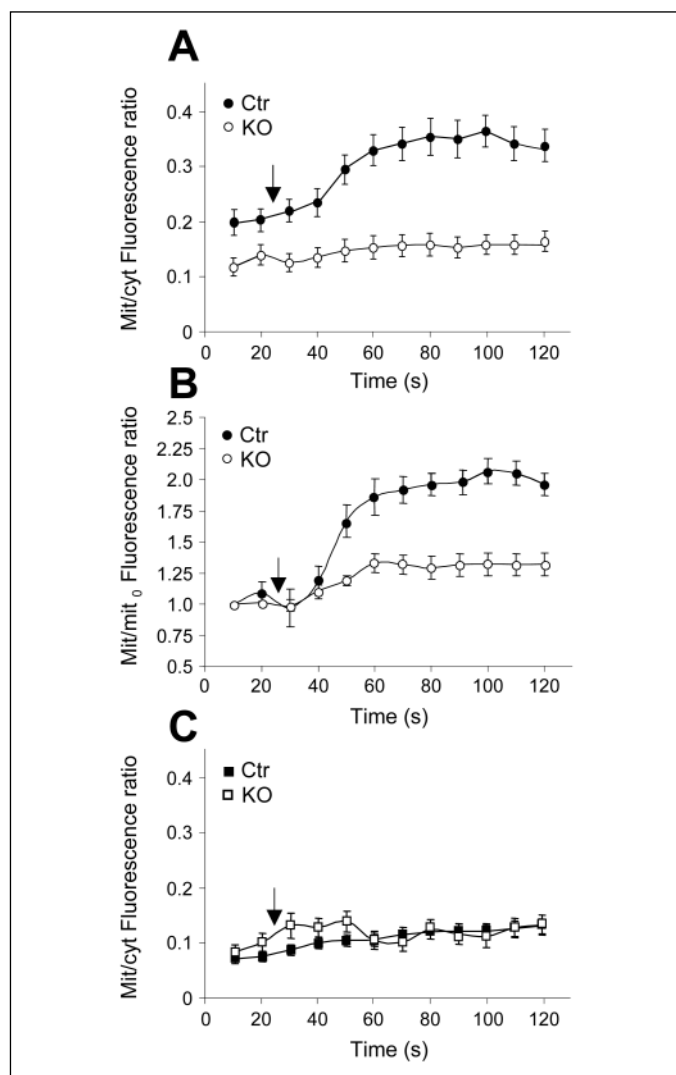


FIGURE 3. Lactate- and pyruvate-induced NAD(P)H responses in control and aralar-deficient neurons. *A*, control (closed symbols) and aralar-deficient neuronal cultures (open symbols) derived from littermate embryos were preincubated in glucose-free HCSS, 1 mM CaCl_2 for 1 h at 37 °C, switched to Ca^{2+} - and glucose-free HCSS (100 μM EGTA), and exposed to 20 mM lactate plus 5 mM malate (LM) (added at the arrow). The changes in mitochondrial/cytosolic NAD(P)H fluorescence were computed within 18 regions containing 4–10 neurons/region. In controls, but not in aralar-deficient neurons, mit/cyt fluorescence ratios were greater than that at $t = 0$ ($p < 0.0001$, one-way ANOVA; from 60 s after LM addition onward, $p < 0.05$, Bonferroni's test). Time course data sets of mit/cyt NAD(P)H ratios from control and aralar-deficient neurons were compared ($p < 0.0001$, two-factor factorial ANOVA). *B*, time course data sets of normalized mitochondrial (mit/mit₀) fluorescence ratios from control and aralar-deficient neurons were also analyzed ($p < 0.0001$, two-factor factorial ANOVA). *C*, aralar-deficient and control neuronal cultures derived from littermate embryos were preincubated as above and exposed to 2 mM pyruvate + 5 mM malate (PM) (squares) (added at the arrow), and the changes in mitochondrial/cytosolic NAD(P)H fluorescence ratios were computed.

in Ca^{2+} uptake by mitochondria and subsequent dehydrogenase activation (8). In the second case, the small Ca^{2+} signals generated by agonist addition were expected to remain below the activation threshold of the mitochondrial Ca^{2+} uniporter but still capable of activating the aralar-MAS pathway.

Fig. 4A shows the increase in mitochondrial NAD(P)H obtained when LM was added together with 60 mM KCl and in the presence of 1 mM external Ca^{2+} in control and aralar-deficient neurons. There was no difference between the increases in $[\text{Ca}^{2+}]_i$ and $[\text{Ca}^{2+}]_{\text{mit}}$ obtained after LM + KCl addition in control and aralar-deficient neurons, in agreement with the lack of effect of aralar overexpression on Ca^{2+} homeostatic mechanisms reported earlier (42) (Fig. 4, *B* and *C*). The increase in

the mit/cyt NAD(P)H fluorescence ratio obtained in the presence of KCl (Fig. 4, *D* and *E*) was significantly larger than that obtained by LM addition itself both in control and aralar-deficient neurons ($p \leq 0.0001$). Reducing equivalent transfer within 40–70 s after LM or LM + KCl addition was 1.89 ± 0.09 and 3.35 ± 0.35 , respectively, in control neurons ($n = 30$ –100, $p < 0.0001$) or 1.34 ± 0.16 and 2.77 ± 0.4 in aralar-deficient neurons ($n = 30$ –100 neurons, $p < 0.0019$). Furthermore, the time course of the response to LM + KCl was the same in control and aralar-deficient neurons ($p = 0.397$).

To verify that the lack of difference between wild-type and aralar-deficient neurons was not due to NAD(P)H being maximally reduced in both cases, we compared the increases in mitochondria/cytosol NAD(P)H ratios obtained with LM plus high K^+ with the NAD(P)H signals in mitochondria obtained in response to rotenone. By inhibiting electron flow through complex I, the addition of 2 μM rotenone plus LM induced a progressive increase in reducing equivalent transfer to mitochondria, as observed previously (13). The quotient between final and initial mit/cyt NAD(P)H ratio obtained after 2 min incubation with rotenone was 8.32 ± 0.62 ($n = 36$ –90 neurons), *i.e.* substantially larger than those observed with LM plus high K^+ .

The increase in mitochondrial NAD(P)H obtained with LM plus high K^+ is expected to result from the additive effects of Ca^{2+} activation of MAS activity and Ca^{2+} activation of mitochondrial dehydrogenases. The lack of differences in mitochondrial NAD(P)H increase between wild-type and aralar-deficient neurons under conditions appropriate for Ca^{2+} uniporter signaling indicates that MAS activity contributes very little, if at all, to this process, suggesting that MAS activity may be inhibited under conditions allowing mitochondrial Ca^{2+} uptake.

By studying MAS activity in isolated mitochondria in the presence or absence of 200 nM RR (Fig. 4F), it was observed that Ca^{2+} activation of MAS was abolished if no RR was present. At this RR concentration, Ca^{2+} uptake in brain mitochondria was fully inhibited (Fig. 4G). These results indicate that Ca^{2+} activation of MAS is blocked if the Ca^{2+} uniporter is active and Ca^{2+} is allowed to enter the mitochondria. We believe that this is because of the effect of mitochondrial Ca^{2+} on the affinity for $\alpha\text{-KG}$ of $\alpha\text{-KGDH}$. This Krebs cycle dehydrogenase and the $\alpha\text{-KG}$ -malate carrier (OGC) compete for the substrate $\alpha\text{-KG}$ (Fig. 1E), so that Ca^{2+} activation of $\alpha\text{-KGDH}$ activity results in an increased affinity for $\alpha\text{-KG}$ and a decrease in $\alpha\text{-KG}$ efflux from mitochondria that would immediately oppose MAS activation, as shown by O'Donnell *et al.* (43, 44).

Regulation of Reducing Equivalent Transfer to Mitochondria by Small Ca^{2+} Signals—Lalo and Kostyuk (45) showed that ATP activation of metabotropic P2Y receptors present in neonatal neurons in a Ca^{2+} -free medium results in small $[\text{Ca}^{2+}]_i$ transients. To study the effect of small $[\text{Ca}^{2+}]_i$ signals on MAS activity, neurons incubated in Ca^{2+} -free HCSS plus 100 μM EGTA were exposed to LM together with 100 μM ATP or different Ca^{2+} -mobilizing agonists. In our neuronal cultures, ATP-induced $[\text{Ca}^{2+}]_i$ transients were much smaller than those obtained with high K^+ , with departures of ≤ 100 nM from resting values that lasted 1 min at most (Fig. 5A); these transients were not accompanied by any detectable increase in $[\text{Ca}^{2+}]_{\text{mit}}$ in control or aralar-deficient neurons (Fig. 5B). Therefore, $[\text{Ca}^{2+}]_{\text{mit}}$ variations are below the detection limit of rhod-2 (dissociation constant (K_d) determined *in situ* in 1.3 μM mitochondria (46), which is somewhat lower than that of fura-2 (K_d 0.2 μM). However, this small Ca^{2+} signal resulted in a remarkable potentiation of LM-dependent increase in mitochondrial NAD(P)H fluorescence in control neurons (Fig. 5, *C* and *D*), which was notably absent in aralar-deficient neurons (Fig. 5, *C* and *E*). In control neurons, reducing equivalent transfer at 80 s after LM + ATP addition was 2.88 ± 0.076 , and

FIGURE 4. Effect of high K^+ depolarization on lactate-induced increase in mitochondrial NAD(P)H fluorescence and malate-aspartate shuttle activity. *A*, NAD(P)H fluorescence images from control (*Ctrl*) and aralar-deficient (*KO*) neurons incubated in glucose-free HCSS, 1 mM CaCl_2 before (*Ctrl-KCl* and *KO-KCl*) and 60 s after LM + 60 mM KCl (*Ctrl+KCl* and *KO+KCl*) administration. *Bar* represents 20 μm . *B* and *C*, $[\text{Ca}^{2+}]_i$ imaging (*B*) and mitochondrial Ca^{2+} dynamics (*C*) of the responses to LM + KCl in fura-2 (*B*) or rhod-2-loaded (*C*) cortical neuronal cultures from control (*Ctrl*) and aralar-deficient (*KO*) mice. LM + KCl were added at the arrows. Each trace represents recordings from a single neuron. *D* and *E*, increase in mitochondrial/cytosolic NAD(P)H fluorescence ratio in control (*D*, closed symbols) or aralar-deficient (*E*, open symbols) neurons from littermate embryos after the addition of LM + KCl (the arrow indicates the time of addition). Each trace corresponds to a group of cells. In both genotypes, LM + KCl induced a significant increase in mit/cyt fluorescence ratios, as compared with their corresponding LM time courses ($p < 0.0001$, two-factor factorial ANOVA). *F*, MAS activity in mouse brain mitochondrial fractions measured at different free Ca^{2+} concentrations in the presence (open bars) or absence (closed bars) of 200 nM ruthenium red (RR). Data are means of two independent experiments performed in triplicate. Differences from 0 Ca^{2+} were significant where indicated. *, $p < 0.01$; **, $p < 0.001$; ***, $p < 0.0001$ (unpaired two-tailed *t* test). *G*, Ca^{2+} uptake in mouse brain mitochondrial fractions. Serial additions of 20 μM Ca^{2+} at 5-min intervals were made. Trace *a*, 200 nM RR were added at the arrow; trace *b*, no RR was added; trace *c*, RR was present from the beginning. The results were unchanged when skeletal muscle mitochondria was used (data not shown).

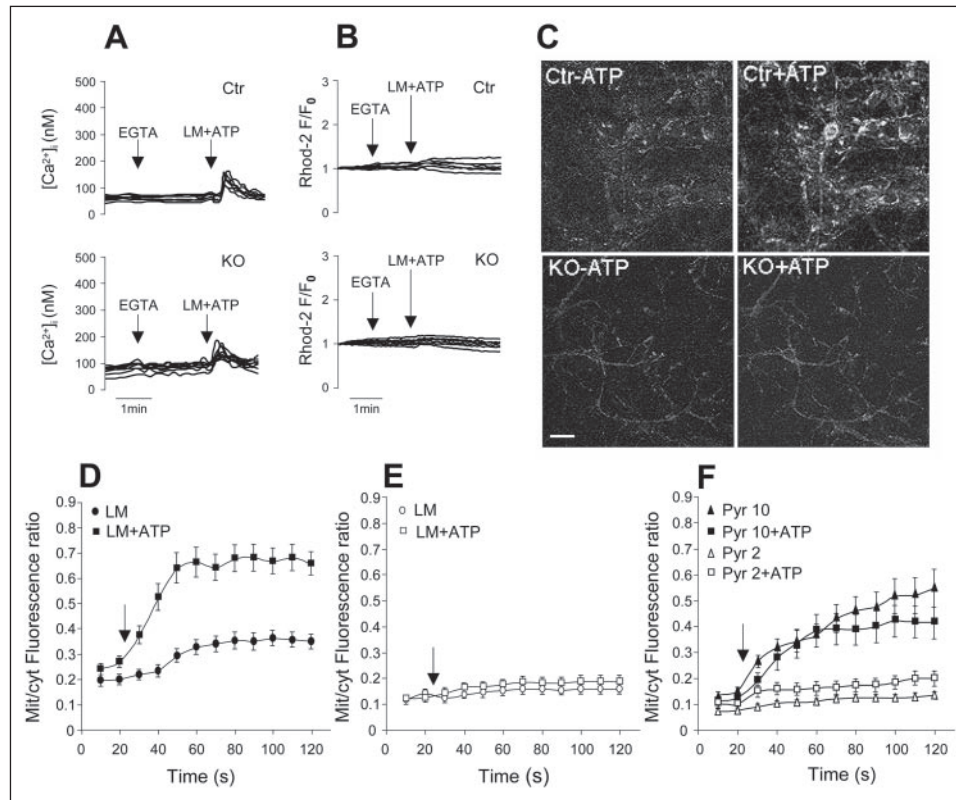
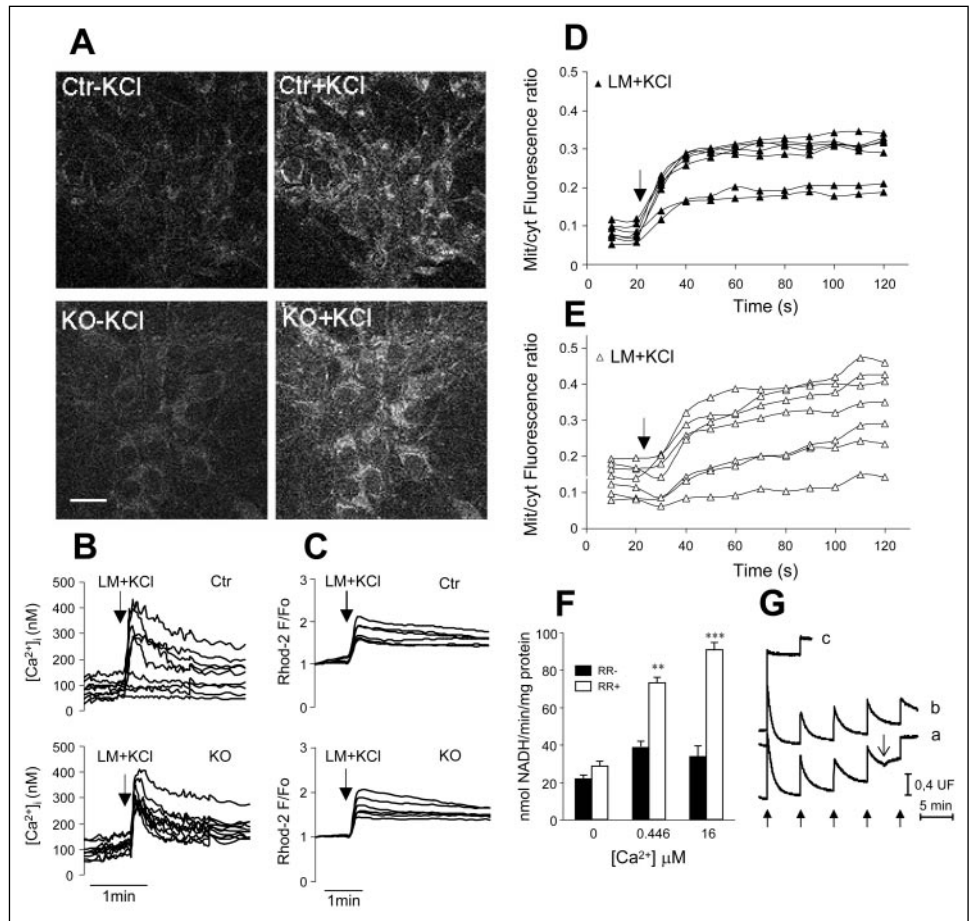


FIGURE 5. Effect of small Ca^{2+} signals on lactate-induced increase in mitochondrial NAD(P)H fluorescence. *A*, $[\text{Ca}^{2+}]_i$ imaging of fura-2-loaded cortical neuronal cultures from control (*Ctrl*) and aralar-deficient (*KO*) mice, exposed to LM + ATP in Ca^{2+} -free HCSS in the presence of 100 μM EGTA. LM + ATP were added at the arrows. Each trace represents the $[\text{Ca}^{2+}]_i$ from a single neuron. *B*, mitochondrial Ca^{2+} dynamics of the responses to LM + ATP in rhod-2-loaded cortical neuronal cultures from control (*Ctrl*) and aralar-deficient (*KO*) mice. *C*, NAD(P)H fluorescence images corresponding to control (*Ctrl-ATP*) and aralar-deficient (*KO-ATP*) neurons before (*Ctrl-ATP* and *KO-ATP*) or 80 s after LM + ATP addition (*Ctrl+ATP* and *KO+ATP*). *Bar* represents 20 μm . *D-E*, control (*D*) or aralar-deficient (*E*) neurons from littermate embryos were preincubated in glucose-free HCSS, 1 mM CaCl_2 for 1 h at 37 $^{\circ}\text{C}$ and switched to Ca^{2+} - and glucose-free HCSS with 100 μM EGTA and LM (circles) or LM + 100 μM ATP (LM + ATP, squares) added at the arrow. Results correspond to mitochondrial/cytosolic NAD(P)H fluorescence ratios (means \pm S.E. values) of 72–180 and 50–120 cells in control and aralar-deficient groups, respectively. Differences in mit/cyt NAD(P)H fluorescence ratios between incubations in the absence or presence of ATP were significant in control cells (D ; $p < 0.0001$, two-factor factorial ANOVA) but not in aralar-deficient (*E*) neurons. *F*, changes in mitochondrial/cytosolic NAD(P)H fluorescence ratio in control neurons after the addition of 2 mM pyruvate + 5 mM malate (*Pyr 2*) or 2 mM pyruvate + 100 μM ATP (*Pyr 2+ATP*), 10 mM pyruvate + 5 mM malate (*Pyr 10*), or 10 mM pyruvate + 100 μM ATP (*Pyr 10+ATP*), in Ca^{2+} -free HCSS in the presence of 100 μM EGTA (the arrow indicates the time of addition).

Aralar Transduces Small Ca^{2+} Signals to Mitochondria

that obtained in the absence of ATP was 1.99 ± 0.15 ($p < 0.0001$), whereas ATP did not modify the responses to LM in aralar-deficient cells (1.38 ± 0.10 versus 1.63 ± 0.15 , in the absence or presence of ATP, $p = 0.16$). Other Ca^{2+} -mobilizing agonists, such as carbachol ($50 \mu\text{M}$) or thapsigargin ($1 \mu\text{M}$), also potentiated in a significant way the response to LM in control neurons (two-factor factorial ANOVA, $p < 0.0001$). Reducing equivalent transfer at 80 s after LM addition was increased in the presence of carbachol (2.68 ± 0.2 versus 2.07 ± 0.15 , $n = 72$ –180 neurons, $p = 0.02$) and thapsigargin (2.35 ± 0.13 versus 1.92 ± 0.17 , $n = 44$ –110 neurons, $p = 0.03$).

Because lactate-derived pyruvate contributes to NAD(P)H generation, we have tested whether the effects of ATP involve Ca^{2+} -stimulated pyruvate metabolism rather than Ca^{2+} -stimulated MAS activity. Fig. 5F shows that the small $[\text{Ca}^{2+}]_i$ signals triggered by ATP had no effect on the increase in mitochondrial NAD(P)H induced by pyruvate. Therefore, these results clearly showed that the neuronal aralar-MAS pathway is selectively activated by small Ca^{2+} signals, below the threshold for Ca^{2+} uniporter activation.

DISCUSSION

Our results show that brain mitochondria have a Ca^{2+} -dependent malate-aspartate NADH shuttle activated by low extramitochondrial Ca^{2+} concentrations, with an $S_{0.5}$ for Ca^{2+} of 324 nM. In neurons, this property is exploited to transduce Ca^{2+} signals to mitochondria via the aralar-MAS pathway, by transferring NAD(P)H reducing equivalents from the cytosol. Quite remarkably, we find that small $[\text{Ca}^{2+}]_i$ signals activate MAS activity under conditions where Ca^{2+} uptake in mitochondria is not observed. Moreover, these same $[\text{Ca}^{2+}]_i$ signals do not activate the pyruvate-dependent reduction of NAD(P)H in mitochondria, a process dependent on the activity of the Ca^{2+} uniporter. We have observed that synaptosomal mitochondria start taking up Ca^{2+} at a global $[\text{Ca}^{2+}]_i$ of about 350–400 nM (27). Clearly, Ca^{2+} signaling through the aralar-MAS pathway in neuronal mitochondria, with an $S_{0.5}$ of 324 nM, would be only significant below these Ca^{2+} concentrations, which is exactly what we found. Our results show for the first time that mitochondria respond to $[\text{Ca}^{2+}]_i$ signals with a substantial increase in NAD(P)H through a Ca^{2+} uniporter-independent pathway.

The Ca^{2+} uniporter-dehydrogenase signaling pathway results in a large activation of mitochondrial dehydrogenases (Ca^{2+} activation of about 4–5-fold for pyruvate dehydrogenase and α -KGDH) (47, 48). However, Ca^{2+} activation of MAS is smaller (3-fold activation in brain mitochondria). Moreover, in the mitochondrial matrix three dehydrogenases are activated by Ca^{2+} , whereas only one (malate dehydrogenase) is activated by the aralar-MAS pathway. It was very surprising to find that the magnitude of the response via the aralar-MAS pathway is very large in neurons, in fact not far from that evoked by the activity of the Ca^{2+} uniporter-dehydrogenases pathway.

Ca^{2+} Activation of Malate-Aspartate NADH Shuttle in Neurons—Lactate is produced by astrocytes and taken up by neurons that use it as an oxidizable substrate, particularly during periods of high activity (49–52). When neurons are supplied with lactate, cytosolic NAD(P)H levels increase, and reducing equivalents are immediately transferred to mitochondria via the aralar-MAS pathway. In the absence of aralar, mitochondrial NAD(P)H levels show a very small increase, which may be attributed to mitochondrial metabolism of lactate-derived pyruvate. Thus, during lactate utilization in resting conditions, most of the transfer of reducing equivalents to mitochondria (about 60%) is carried out by MAS activity.

Small $[\text{Ca}^{2+}]_i$ signals evoked by agonists that, by themselves, do not stimulate mitochondrial Ca^{2+} uptake and dehydrogenase activity selec-

tively activate the aralar-MAS pathway so that reducing equivalent transfer to mitochondria is now strongly potentiated. ATP and carbachol applied in Ca^{2+} -free media behave this way in neurons and result in about 3-fold MAS activation (the difference between reducing equivalent transfer values in control and aralar-deficient neurons, at 50–70 s after LM addition in the absence or presence of ATP). This activation is close to the maximal activation of MAS observed in isolated mitochondria (about 3-fold). However, the ATP-evoked $[\text{Ca}^{2+}]_i$ transients only reach 200 nM at best, clearly below the Ca^{2+} concentrations required to fully activate MAS in brain mitochondria (about $1 \mu\text{M}$; Fig. 1). This implies a close proximity between mitochondrial aralar and the IP_3 receptors, the Ca^{2+} release sites activated by ATP, so that localized Ca^{2+} concentrations, higher than those of the bulk cytosol, could exist and result in full activation of MAS. However, these local Ca^{2+} concentrations would still be unable to activate the Ca^{2+} uniporter-dehydrogenase pathway.

Neurotransmitters (glutamate and acetylcholine) and/or neuro-modulators (histamine, adenosine, and neurotrophin-3) acting on G-protein-coupled receptors or Trk receptors activate phospholipase C isoenzymes resulting in different dynamics of IP_3 production and diverse $[\text{Ca}^{2+}]_i$ transients (53–56). This variability may arise from the engagement of different G-proteins and phospholipase C isoforms in a cell-specific manner. IP_3 -dependent Ca^{2+} mobilization is critically involved in neuromodulation, as it controls excitability, transmitter release, and gene expression (53–55) in a cell- and receptor-specific way. Agonists that evoke IP_3 production may produce quite different $[\text{Ca}^{2+}]_i$ and $[\text{Ca}^{2+}]_{\text{mit}}$ transients, depending on the specific receptor being activated and agonist concentration (57, 56), and some may produce small $[\text{Ca}^{2+}]_i$ transients that selectively activate the aralar-MAS pathway in neuronal mitochondria. The energization obtained by Ca^{2+} activation of MAS can be utilized to produce more ATP in mitochondria, as found in studies with aralar-overexpressing cells (42). Indeed, preliminary data indicate that lactate supply during mild hypoglycemia increases ATP levels in neurons and even more so in the presence of nonhydrolyzable ATP agonists, but none of these effects were observed in aralar-deficient neurons.⁶ Further consequences of this energization have yet to be explored, but it is tempting to suggest that it could prime mitochondria for subsequent energy-requiring processes such as metabolite transport, etc., that may be involved in the final response to the neuromodulator.

Activity-dependent changes in the NAD(P)/NAD(P)H ratio have been detected long ago in different cell types (58). In neurons and synaptosomes, high K^+ depolarization leads to an initial transient drop in NAD(P)H that is followed by an increase in NAD(P)H (8). Similar changes are produced by neural activity (12, 13, 52, 59, 60). These changes have been attributed to physiological increases in $[\text{Ca}^{2+}]_i$ and Ca^{2+} (and possibly ADP) entry in mitochondria leading to the following: 1) increased respiration and mitochondrial NADH oxidation, and 2) Ca^{2+} activation of mitochondrial dehydrogenases resulting in NADH reduction, whereas Shuttleworth *et al.* (13) found that they were Ca^{2+} -independent. In our experimental conditions, the transient decrease in mitochondrial NAD(P)H was not observed, possibly because the imaging rate was too slow, and lactate was added together with high K^+ . However, a rapid increase in mitochondrial NAD(P)H in response to high K^+ stimulation was clearly shown, and this was not modified by aralar deficiency, in agreement with the notion that it involves the Ca^{2+} uniporter signaling pathway.

⁶ B. Pardo and J. Satrústegui, unpublished observations.

Indeed, our results show that MAS activity in neuronal mitochondria is superseded under conditions where high $[\text{Ca}^{2+}]_i$ signals drive Ca^{2+} uniporter activity. This is probably because of competition for substrate between α -KGDH of Krebs cycle and the α -KG-malate transporter (OGC) of MAS. The two reactions compete for α -KG by virtue of their apparent K_m values. The K_m value for α -KG of the OGC on the matrix side of the carrier is 1.5 mM (61) and that of α -KGDH is around 0.2 mM (47). Activation by Ca^{2+} of α -KGDH increases its affinity for α -KG (7, 47), causing a reduction in OGC activity (43) and an inhibition of MAS activity (44). Although this effect is present within the whole time window of our experiments (about 1.5 min), it could disappear when the activation by Ca^{2+} of α -KGDH comes to an end. Thus, it is possible that after the decay of $[\text{Ca}^{2+}]_{\text{mit}}$ transients, MAS activity could prolong the increase in mitochondrial NAD(P)H induced by high $[\text{Ca}^{2+}]_i$ signals and thus contribute to ATP synthesis and recovery of the resting state, conditions that rely on neuronal lactate utilization (62).

It should be noted that the increase in mitochondrial NAD(P)H obtained through the aralar-MAS pathway does not require the presence of Ca^{2+} in the mitochondrial matrix, an event that contributes to cell death in a number of cell types (63), including neurons (64). It may also provide an alternative mechanism to supply mitochondrial NADH under oxidative stress conditions, where α -KGDH is selectively inhibited (65). Lactate, and not glucose, is the major neuronal energy substrate after an insult, and overexpression of a lactate transporter in neurons enhances neuronal resistance to excitotoxicity (66), suggesting that the aralar-MAS pathway might also enhance survival to glutamate excitotoxicity.

Acknowledgments—We thank Dr. A. Martínez-Serrano and Dr. J. M. Cuezva for helpful advice and critical reading of the manuscript. We also thank Barbara Sesé, Inmaculada Ocaña, and Juliana Sánchez García for excellent technical assistance.

REFERENCES

- Gunter, T. E., Yule, D. I., Gunter, K. K., Eliseev, R. A., and Salter, J. D. (2004) *FEBS Lett.* **567**, 96–102
- Kirichok, Y., Krapivinsky, G., and Clapham, D. E. (2004) *Nature* **427**, 360–364
- Rizzuto, R., Pinton, P., Carrington, W., Fay, F. S., Fogarty, K. E., Lifshitz, L. M., Tuft, R. A., and Pozzan, T. (1998) *Science* **280**, 1763–1766
- Gilbert, J. A., and Parekh, A. B. (2000) *EMBO J.* **19**, 6401–6407
- Montero, M., Alonso, M. T., Carnicero, E., Cuchillo-Ibanez, I., Albillos, A., Garcia, A. G., Garcia-Sancho, J., and Alvarez, J. (2000) *Nat. Cell Biol.* **2**, 57–61
- Filippin, L., Magalhaes, P. J., Di Benedetto, G., Colella, M., and Pozzan, T. (2003) *J. Biol. Chem.* **278**, 39224–39234
- Nichols, B. J., and Denton, R. M. (1995) *Mol. Cell. Biochem.* **149**, 203–212
- Duchen, M. R. (1992) *Biochem. J.* **283**, 41–50
- Brandes, R., and Bers, D. M. (1999) *Biophys. J.* **77**, 1666–1682
- Nicholls, D. G., and Budd, S. L. (2000) *Physiol. Rev.* **80**, 315–360
- Voronina, S., Sukhomlin, T., Johnson, P. R., Erdemli, G., Petersen, O. H., and Tepikin, A. (2002) *J. Physiol. (Lond.)* **539**, 41–52
- Kann, O., Schuchmann, S., Buchheim, K., and Heinemann, U. (2003) *Neuroscience* **119**, 87–100
- Shuttleworth, C. W., Brennan, A. M., and Connor, J. A. (2003) *J. Neurosci.* **23**, 3196–3208
- Pralong, W. F., Spat, A., and Wollheim, C. B. (1994) *J. Biol. Chem.* **269**, 27310–27314
- Hajnóczky, G., Robb-Gaspers, L. D., Seitz, M. B., and Thomas, A. P. (1995) *Cell* **82**, 415–424
- Robb-Gaspers, L. D., Burnett, P., Rutter, G. A., Denton, R. M., Rizzuto, R., and Thomas, A. P. (1998) *EMBO J.* **17**, 4987–5000
- Pitter, J. G., Szanda, G., Duchen, M. R., and Spat, A. (2005) *Cell Calcium* **37**, 35–44
- del Arco, A., and Satrustegui, J. (1998) *J. Biol. Chem.* **273**, 23327–23334
- del Arco, A., Agudo, M., and Satrustegui, J. (2000) *Biochem. J.* **345**, 725–732
- Palmieri, L., Pardo, B., Lasorsa, F. M., del Arco, A., Kobayashi, K., Iijima, M., Runswick, M. J., Walker, J. E., Saheki, T., Satrustegui, J., and Palmieri, F. (2001) *EMBO J.* **20**, 5060–5069
- LaNoue, K. F., Meijer, A. J., and Brouwer, A. (1974) *Arch. Biochem. Biophys.* **161**, 544–550
- del Arco, A., Morcillo, J., Martínez-Morales, J. R., Galian, C., Martos, V., Bovolenta, P., and Satrustegui, J. (2002) *Eur. J. Biochem.* **269**, 3313–3320
- Ramos, M., del Arco, A., Pardo, B., Martínez-Serrano, A., Martínez-Morales, J. R., Kobayashi, K., Yasuda, T., Bogonez, E., Bovolenta, P., Saheki, T., and Satrustegui, J. (2003) *Brain Res. Dev. Brain Res.* **143**, 33–46
- Roesch, K., Hynds, P. J., Varga, R., Tranebjærg, L., and Koehler, C. M. (2004) *Hum. Mol. Genet.* **13**, 2101–2111
- Ramos, N., Reichert, J. G., Smith, C. J., Silverman, J. M., Bespalova, I. N., Davis, K. L., and Buxbaum, J. D. (2004) *Am. J. Psychiatry* **161**, 662–669
- Jalil, M. A., Begum, L., Contreras, L., Pardo, B., Iijima, M., Li, M. X., Ramos, M., Marmol, P., Horiuchi, M., Shimotsu, K., Nakagawa, S., Okubo, A., Sameshima, M., Isashiki, Y., del Arco, A., Kobayashi, K., Satrustegui, J., Saheki, T. (2005) *J. Biol. Chem.* **280**, 31333–31339
- Martínez-Serrano, A., and Satrustegui, J. (1992) *Mol. Biol. Cell* **3**, 235–248
- Rolfe, D. F., Hulbert, A. J., and Brand, M. D. (1994) *Biochim. Biophys. Acta* **1188**, 405–416
- Gryniewicz, G., Poenie, M., and Tsien, R. Y. (1985) *J. Biol. Chem.* **260**, 3440–3450
- Ruiz, F., Alvarez, G., Pereira, R., Hernandez, M., Villalba, M., Cruz, F., Cerdan, S., Bogonez, E., and Satrustegui, J. (1998) *Neuroreport* **9**, 1277–1282
- Brewer, G. J., Torricelli, J. R., Evege, E. K., and Price, P. J. (1993) *J. Neurosci. Res.* **35**, 567–576
- Ruiz, F., Alvarez, G., Ramos, M., Hernandez, M., Bogonez, E., and Satrustegui, J. (2000) *Eur. J. Pharmacol.* **404**, 29–39
- Patterson, G. H., Knobel, S. M., Arkhammar, P., Thastrup, O., and Piston, D. W. (2000) *Proc. Natl. Acad. Sci. U. S. A.* **97**, 5203–5207
- Rocheleau, J. V., Head, W. S., Nicholson, W. E., Powers, A. C., and Piston, D. W. (2002) *J. Biol. Chem.* **277**, 30914–30920
- Passonneau, J. V., and Lowry, O. H. (1974) in *Methods of Enzymatic Analysis* (Bergmeyer, H. U., ed) 2nd Ed., pp. 1452–1456, Academic Press, New York
- Sinasac, D. S., Moriyama, M., Jalil, M. A., Begum, L., Li, M. X., Iijima, M., Horiuchi, M., Robinson, B. H., Kobayashi, K., Saheki, T., and Tsui, L. C. (2004) *Mol. Cell. Biol.* **24**, 527–536
- Gunter, K. K., and Gunter, T. E. (1994) *J. Bioenerg. Biomembr.* **26**, 471–485
- Broer, S., Rahman, B., Pellegrini, G., Pellerin, L., Martin, J. L., Verleysdonk, S., Hamprecht, B., and Magistretti, P. J. (1997) *J. Biol. Chem.* **272**, 30096–30102
- Chance, B., and Baltscheffsky, H. (1958) *J. Biol. Chem.* **233**, 736–739
- Avi-Dor, Y., Olson, J. M., Doherty, M. D., and Kaplan, N. O. (1962) *J. Biol. Chem.* **237**, 2377–2383
- Nguyen, N. H., Brathe, A., and Hassel, B. (2003) *J. Neurochem.* **85**, 831–842
- Lasorsa, F. M., Pinton, P., Palmieri, L., Fiermonte, G., Rizzuto, R., and Palmieri, F. (2003) *J. Biol. Chem.* **278**, 38686–38692
- O'Donnell, J. M., Doumen, C., LaNoue, K. F., White, L. T., Yu, X., Alpert, N. M., and Lewandowski, E. D. (1998) *Am. J. Physiol.* **274**, H467–H476
- O'Donnell, J. M., Kudej, R. K., LaNoue, K. F., Vatner, S. F., and Lewandowski, E. D. (2004) *Am. J. Physiol.* **286**, H2237–H2242
- Lalo, U., and Kostyuk, P. (1998) *Brain Res. Dev. Brain Res.* **111**, 43–50
- Collins, T. J., Lipp, P., Berridge, M. J., and Bootman, M. D. (2001) *J. Biol. Chem.* **276**, 26411–26420
- Rutter, G. A., and Denton, R. M. (1988) *Biochem. J.* **252**, 181–189
- McCormack, J. G., Bromidge, E. S., and Dawes, N. J. (1988) *Biochim. Biophys. Acta* **934**, 282–292
- Vicario, C., Arizmendi, C., Malloch, G., Clark, J. B., and Medina, J. M. (1991) *J. Neurochem.* **57**, 1700–1707
- Pellerin, L., and Magistretti, P. J. (1994) *Proc. Natl. Acad. Sci. U. S. A.* **91**, 10625–10629
- Pellerin, L. (2003) *Neurochem. Int.* **43**, 331–338
- Kasischke, K. A., Vishwasrao, H. D., Fisher, P. J., Zipfel, W. R., and Webb, W. W. (2004) *Science* **305**, 99–103
- Li, Z., Miyata, S., and Hatton, G. I. (1999) *Neuroscience* **93**, 667–674
- He, X., Yang, F., Xie, Z., and Lu, B. (2000) *J. Cell Biol.* **149**, 783–792
- Basheer, R., Arrigoni, E., Thatte, H. S., Greene, R. W., Ambudkar, I. S., and McCarley, R. W. (2002) *J. Neurosci.* **22**, 7680–7686
- Berridge, M. J., Bootman, M. D., and Roderick, H. L. (2003) *Nat. Rev. Mol. Cell Biol.* **4**, 517–529
- Monteith, G. R., and Blaustein, M. P. (1999) *Am. J. Physiol.* **276**, C1193–C1204
- Chance, B., Cohen, P., Jobsis, F., and Schoener, B. (1962) *Science* **137**, 499–508
- Mironov, S. L., and Richter, D. W. (2001) *J. Physiol. (Lond.)* **533**, 227–236
- Hayakawa, Y., Nemoto, T., Iino, M., and Kasai, H. (2005) *Cell Calcium* **37**, 359–370
- Sluse, F. E., Goffart, G., and Liebecq, C. (1973) *Eur. J. Biochem.* **32**, 283–291
- Pellerin, L., and Magistretti, P. J. (2004) *Science* **305**, 50–52
- Rizzuto, R., Pinton, P., Ferrari, D., Chami, M., Szabadkai, G., Magalhaes, P. J., Di Virgilio, F., and Pozzan, T. (2003) *Oncogene* **22**, 8619–8627
- Stout, A. K., Raphael, H. M., Kanterewicz, B. L., Klann, E., and Reynolds, I. J. (1998) *Nat. Neurosci.* **1**, 366–373
- Tretter, L., and Adam-Vizi, V. (2000) *J. Neurosci.* **20**, 8972–8979
- Bliss, T. M., Ip, M., Cheng, E., Minami, M., Pellerin, L., Magistretti, P., and Sapolsky, R. M. (2004) *J. Neurosci.* **24**, 6202–6208